The angiogenic response to PLL-g-PEG-mediated HIF-1 plasmid DNA delivery in healthy and diabetic rats

Thiersch, Markus ; Rimann, Markus ; Panagiotopoulou, Vasiliki ; Öztürk, Ece ; Biedermann, Thomas ; Textor, Marcus ; Lühmann, Tessa C ; Hall, Heike

Abstract: Impaired angiogenesis is a major clinical problem and affects wound healing especially in diabetic patients. Improving angiogenesis is a reasonable strategy to increase diabetes-impaired wound healing. Recently, our lab described a system of transient gene expression due to pegylated poly-l-lysine (PLL-g-PEG) polymer-mediated plasmid DNA delivery in vitro. Here we synthesized peptide-modified PLL-g-PEG polymers with two functionalities, characterized them in vitro and utilized them in vivo via a fibrin-based delivery matrix to induce dermal wound angiogenesis in diabetic rats. The two peptides were 1) a TG-peptide to covalently bind these nanocondensates to the fibrin matrix (TG-peptide) for a sustained release and 2) a polyR peptide to improve cellular uptake of these nanocondensates. In order to induce angiogenesis in vivo we condensed modified and non-modified polymers with plasmid DNA encoding a truncated form of the therapeutic candidate gene hypoxia-inducible transcription factor 1 (HIF-1). HIF-1 is the primarily oxygen-dependent regulated subunit of the heterodimeric transcription factor HIF-1, which controls angiogenesis among other physiological pathways. The truncated form of HIF-1 lacks the oxygen-dependent degradation domain (ODD) and therefore escapes degradation under normoxic conditions. PLL-g-PEG polymer-mediated HIF-1 -ΔODD plasmid DNA delivery was found to lead to a transiently induced gene expression of angiogenesis-related genes Acta2 and Pecam1 as well as the HIF-1 target gene Vegf in vivo. Furthermore, HIF-1 gene delivery was shown to enhance the number endothelial cells and smooth muscle cells - precursors for mature blood vessels - during wound healing. We show that - depending on the selection of the therapeutic target gene - PLL-g-PEG nanocondensates are a promising alternative to viral DNA delivery approaches, which might pose a risk to health.

DOI: https://doi.org/10.1016/j.biomaterials.2013.02.021

The angiogenic response to PLL-g-PEG-mediated HIF-1alpha plasmid DNA delivery in healthy and diabetic rats

Markus Thiersch[a,b,*], Markus Rimann[a,1], Vasiliki Panagiotopoulou[a,2], Ece Öztürk[a,3], Thomas Biedermann[c], Marcus Textor[d], Tessa C. Lühmann[a,4], Heike Hall[a]

[a]Laboratory for Biologically Oriented Materials, Department of Materials, ETH Zurich, CH-8093, Switzerland

[b]University of Zurich; Institute of Veterinary Physiology; Winterthurerstrasse 260; CH-8057 Zurich, Switzerland

[c]Tissue Biology Research Unit University Children's Hospital Zurich, CH-8008, Switzerland

[d]BioInterface Group, Laboratory for Surface Science and Technology, Department of Materials, ETH Zurich, CH-8093, Switzerland

[*] Corresponding Author:
Markus Thiersch
Email: markus.thiersch@uzh.ch

[1] Now at ZHAW Zurich University of Applied Sciences; Life Sciences und Facility Management; Einsiedlerstrasse 31, 8820 Wädenswil, Switzerland

[2] Now at Zühlke Engineering AG; Wiesenstrasse 10A, 8952 Schlieren, Switzerland

[3] Now at ETH Zurich, Cartilage Engineering and Regeneration, Department of Health Science and Technology, CH-8092, Switzerland

[4] Now at Institute of Pharmacy and Food Chemistry; Chair of Pharmaceutics and Biopharmacy; University Würzburg; Am Hubland; 97074 Würzburg, Germany

Abstract

Impaired angiogenesis is a major clinical problem and affects wound healing especially in diabetic patients. Improving angiogenesis is a reasonable strategy to increase diabetes-impaired wound healing. Recently, our lab described a system of transient gene expression due to pegylated poly-L-lysine (PLL-g-PEG) polymer-mediated plasmid DNA delivery *in vitro*. Here we synthesized peptide-modified PLL-g-PEG polymers with two functionalities, characterized them *in vitro* and utilized them *in vivo* via a fibrin-based delivery matrix to induce dermal wound angiogenesis in diabetic rats. The two peptides were 1) a TG-peptide to covalently bind these nanocondensates to the fibrin matrix (TG-peptide) for a sustained release and 2) a polyR peptide to improve cellular uptake of these nanocondensates. In order to induce angiogenesis *in vivo* we condensed modified and non-modified polymers with plasmid DNA encoding a truncated form of the therapeutic candidate gene hypoxia-inducible transcription factor 1α (HIF-1α). HIF-1α is the primarily oxygen-dependent regulated subunit of the hetero-dimeric transcription factor HIF-1, which controls angiogenesis among other physiological pathways. The truncated form of HIF-1α lacks the oxygen-dependent degradation domain (ODD) and therefore escapes degradation under normoxic conditions. PLL-g-PEG polymer mediated HIF-1α–ΔODD plasmid DNA delivery was found to lead to a transiently induced gene expression of angiogenesis related genes Acta2 and Pecam1 as well as the HIF-1α target gene *Vegf in vivo*. Furthermore, HIF-1α gene delivery was shown to enhance the number endothelial cells and smooth muscle cells – precursors for mature blood vessels – during wound healing. We show that – depending on the selection of the therapeutic target gene – PLL-g-PEG nanocondensates are a promising alternative to viral DNA delivery approaches, which might pose a risk to health.

Keywords:

PLL-g-PEG, DNA Delivery, Wound Healing, Angiogenesis, HIF-1alpha

1. Introduction

Wound healing is a highly dynamic process comprising several overlapping stages: haemostasis/inflammation, migration, proliferation and maturation phases. It involves complex interactions of extracellular (ECM) molecules, soluble mediators, various resident cells and infiltrating cells to achieve the goal of tissue integrity [1]. Diseases such as diabetes mellitus interfere with wound healing by disrupting the orderly sequence of events at one or more of the stages, thereby compromising the wound healing process. The deficiency of endogenous growth factors [2, 3] and/or the excessive production of exudates and expression of high levels of tissue destructive proteinases [4] are associated to chronic wound formation. Diabetic ulcerations are characterized by impaired neovascularization and blood perfusion. Approximately 5 to 15% of diabetes patients are prone to foot ulcer development [5], requiring an appropriate strategy to improve wound healing.

Gene therapy has gained increasing attention as an alternative approach for wound treatment [6-8]. Especially non-viral gene transfer benefits from biosafety and the unlimited gene size transportation capacity [9]. However, the major drawbacks of non-viral vectors are their poor *in vivo* transfection efficiencies resulting in low protein production, as well as their transient gene expression profile, which for improvement of local and temporal wound healing, is desirable. Therapeutic DNA is able to condense with poly-cationic substances such as poly-L-lysine (PLL), poly-L-ornithin or polyethylenimine (PEI) [10-13]. Polymers with high cationic density confer cytotoxicity [14], which is circumvented by the formation of different block-

copolymers between poly(ethylene glycol) (PEG) and PLL, PEI or poly-aspartic acid [10, 13-15]. Polymer-DNA condensates using grafted copolymers of PLL and PEG have been shown to combine low cytotoxicity, stealth properties and high transfection efficiency in COS-7 cells [16, 17], suggesting that they are a promising tool for effective transport and delivery of therapeutic DNA.

An excellent candidate protein to support wound revascularization is the transcription factor hypoxia-inducible factor 1 (HIF-1). Among other physiological pathways, HIF-1 controls angiogenesis by regulating the expression of pro-angiogenic target genes including *Vegf-a* [18]. HIF-1 is an oxygen-responsive, heterodimeric transcription factor consisting of an alpha-subunit and a beta-subunit. In order to quickly react to changes in oxygen concentrations, both subunits are constitutively expressed with HIF-1α being posttranslationally regulated by oxygen availability. Prolylhydroxylases (PHDs) hydroxylate HIF-1α at two specific proline residues that are located in the oxygen-dependent degradation domain (ODD) [19-21] in an oxygen-dependent manner. This targets HIF-1α for the binding of the tumor suppressor von-Hippel-Lindau protein (VHL), which initiates the accumulative binding of ubiquitin and eventually leads to proteasomal degradation of HIF-1α [22]. Additionally, factor inhibiting HIF (FIH) hydroxylates human HIF-1α subunits at an asparagine residue in the C-terminal transactivation domain. This interferes with the binding of the essential transcriptional co-activators p300 and CBP (CREB binding protein) and reduces the transcriptional activity of HIF-1 [23]. An engineered variant of HIF-1α, which lacks the ODD, escapes the oxygen-dependent degradation – resulting in stable expression under normoxic conditions. Recently, condensates of HIF-1α–ΔODD plasmid DNA and peptides were shown to increase the number and the quality of newly formed blood vessels in full thickness excision dermal wounds of healthy mice after release

from modified 3D-fibrin matrices [24]. Fibrin hydrogels harbor a great wound healing potential. They are among the most often used native hydrogels to induce angiogenesis and wound healing *per se* [25, 26] and have been widely used as a drug delivery system [27, 28].

Since the formation of new blood vessels is a prerequisite for successful wound healing, we tested whether PLL-g-PEG based polymers deliver potentially therapeutic HIF-1α−ΔODD plasmid DNA and induce blood vessel formation *in vivo*. Thus, we produced and employed 3D-Fibrin matrices as release system for the local gene therapeutic approach and analyzed the effect of HIF-1α−ΔODD plasmid DNA delivery on wound revascularization under normal and diabetic conditions *in vivo*.

2. Materials and Methods

2.1. Nomenclature of PLL-g-PEG polymers

Three different PLL-g-PEG polymers were used in this study (Fig. 1) consisting of a 20 kDa poly-L-lysine (PLL) backbone grafted with 5 kDa poly(ethylene glycol) (PEG). Grafting density (g) indicates the percentage of pegylated lysine residues. TG and polyR abbreviate peptide sequences encoding either a transglutaminase recognition sequence allowing covalent incorporation of the polymer into fibrin hydrogels (TG-peptide) or a nuclear translocation sequence facilitating nuclear polymer uptake (polyR-peptide).

2.2. PLL-g-PEG polymer synthesis

The synthesis of unmodified PLL_{20}-g_5-PEG_5 was previously described by Pasche and coworkers and by Rimann et al. [17, 29].

For PLL_{20}-g_8-PEG_5-TG synthesis, 26 mg NHS-PEG-Mal (4750 g/mol, IRIS, PEG1063) was mixed with the 29.6 mg N-terminal Fmoc-protected TG peptide NQEQVSPLGYERCG (GenScript Corporation, Piscataway, NJ, USA) in 500 µl DMSO at room temperature. Further, 20 mg PLL_{20} (20 kDa, Sigma, P7890) was dissolved in 90 µM trieethylamine containing DMSO and added drop-wise into the aforementioned solution, allowing a reaction over night at room temperature. After adding 8 ml H_2O the solution was dialyzed against ddH_2O at 4 °C, lyophilized and analyzed by ^{1}H-NMR in D_2O (supplemental data Fig.1). To remove the Fmoc protection, the PLL_{20}-g_8-PEG_5-TG-Fmoc construct was dissolved in 20% piperidine and 80% DMF and reacted at room temperature for 1 h. After adding 17 ml H_2O the product was again dialyzed against H_2O. After filtering and lyophilization the product was verified by ^{1}H-NMR in D_2O (supplemental data Fig.2 I).

PLL_{20}-g_3-PEG_5-polyR was synthesized using 13 mg NHS-PEG-Mal and 10mg PLL_{20} - each dissolved in 0.1 M phosphate buffer. Both solutions were mixed and incubated for 1 h at room temperature. 14.6 mg of the polyR peptide dissolved in phosphate buffer were added and reacted over night at room temperature. The product was dialyzed against water, lyophilized and characterized by ^{1}H-NMR in D_2O (supplemental data Fig.2 II).

2.3. Formulation of PLL-g-PEG-DNA nanocondensates

To form polymer-DNA nanocondensates we used plasmid DNA expressing either EGFP (pEGFP-N1) or a form of HIF-1α lacking the oxygen dependent degradation domain (pHIF-1α–ΔODD). To simplify nomenclature the condensates were given abbreviations (Table 1). As previously described, 1 µg plasmid DNA was condensed with PLL_{20}-g_5-PEG_5 (N/P ratio 3.125) [17]. Likewise, 1 µg plasmid DNA was condensed with PLL_{20}-g_5-PEG_8-TG or PLL_{20}-g_5-PEG_3-polyR with N/P ratios ranging from 1 to 25 in order to find the optimal ratio for transfection. For all subsequent experiments the N/P ratio 6.25 was used. The hydrodynamic diameter of the nanocondensates was determined by dynamic light scattering as previously described [17].

2.4. Cell Culture and *In vitro* Transfection

COS-7 cells were cultured in 1 g/l glucose containing DMEM (Gibco), supplemented with 10% FBS (Sigma) and 1% Pen/Strep (Sigma) at 37°C and 5% CO_2. To mimic a high-glucose environment, cells were adapted to 4.5 g/l glucose containing DMEM medium (Gibco) for 4 weeks [30]. Polymer-DNA condensates were produced and applied as described by Rimann et al. [17].

2.5. Cell Viability Assay

WST-1 assay (Roche) was used to determine the viability of COS-7 cells after transfection with polymeric nanocondensates under normal and high-glucose conditions. Fresh growth medium was added on cells followed by addition of 50 µl WST-1 reagent. After incubation at 37°C for 1 hour, the absorbance was detected by a TECAN Infinite M200 microplate reader at 440 nm wavelength. The cell viability was assessed by normalization to non-treated cells.

2.6. 3D Fibrin Hydrogels

For *in vitro* release assays 200 µl fibrin hydrogels were produced containing 2 mg/ml fibrinogen (Sigma), 1 U/ml factor XIII, 1.25 mM $CaCl_2$ and 5 U/ml thrombin (Sigma). Each fibrin gel contained either 2 µg naked pEGFP-N1 plasmid DNA or nanocondensates with a total amount of 2 µg pEGFP-N1 plasmid DNA. For *in vivo* wound healing studies 100 µl fibrin hydrogels per wound were produced consisting of 10 mg/ml fibrinogen, 2 U/ml factor XIII, 1.25 mM $CaCl_2$ and 7.5 U/ml thrombin. Such hydrogels further contained either 1 µg recombinant human $VEGF_{165}$ (Peprotech), PLL_{20}-g_5-PEG_5/pHIF-1α–ΔODD (-/HIF), PLL_{20}-g_8-PEG_5-TG/pHIF-1α–ΔODD (TG/HIF) or PLL_{20}-g_3-PEG_5-polyR/pHIF-1α–ΔODD (polyR/HIF).

2.7. In vitro release from 3D fibrin hydrogels

Polymer-DNA containing hydrogels were covered with PBS and incubated at 37° C and 5% CO_2 while gently shaking. Nanocondensate release was monitored for 7 days and PBS supernatant was removed and replaced in a 24-hour cycle. To determine the amount of released DNA supernatant were treated with NaOH to release DNA from the positively charged polymers and DNA was quantified by PicoGreen dsDNA reagent (Invitrogen) according to manufactures protocol. To determine the functionality of the released nanocondensates COS-7 cells were incubated with 200 µl

supernatant for 48 hours and transfection efficiency was determined by EGFP expression.

2.8. Animals

Animals were treated in accordance with the regulations of the Swiss Veterinary Authority of Zurich. Sprague Dawley rats (Crl:CD(SD) Charles River, Germany) weighing 180 to 220 g were kept pair wise in a 12 h light/dark cycle at 22°C and 50% humidity. Diabetes mellitus type I was induced by a single, intravenous injection of 65 mg/kg streptozotocin (STZ) (Sigma). Control animals received a Mock-injection of the respective solvent 0.1M sodium citrate buffer (pH 4.5). Blood glucose levels were measured with a glucometer (Roche, Accu-Chek Aviva) by puncturing the tail tip. Blood glucose levels higher than 16.7 mM 3 days after injection were considered to be diabetic. STZ-treated animals with blood glucose levels below 16.7 mM received a second injection of STZ.

2.9. Full-thickness excision wound preparation

1 week after receiving STZ- or Mock-injection rats were anesthetized by isoflurane (Attane, Minrad Inc., Buffalo, USA) and received a single 5 mg/kg subcutaneous injection of Carprofen (Rimadyl, Pfizer AG, Zurich, Switzerland). After shaving the dorsal region, 10 mm diameter full-thickness wounds were generated with a small round scissor. The wounds were filled with 100 µl fibrin hydrogel containing $VEGF_{165}$ or nanocondensates. Fibrin-only hydrogels served as negative control. Fibrin hydrogels were covered with a dressing (Opsite Flexigrad, Smith & Nephew) and fixed with a tape (Leukotape Claassic, Smith & Nephew). Animals were sacrificed 3 and 7 days post injury by pneumothorax generation with prior anesthesia in 4% isoflurane. Wounds were isolated and bisected. One half was immediately frozen in liquid nitrogen for RNA and protein isolation. The second half was fixed by 4% PFA

(Acros Organics) in MB buffer (65 mM PIPESm, 25 mM HEPES, 10 mM EGTA, 3 mM $CaCl_2$, pH 6.9) for 24 hours. For immunohistological analyses wounds were embedded in paraffin and cut into 7 µm sections.

2.10. Immunohistological Analyzes

Paraffin sections were rehydrated followed by an antigen-retrieval treatment in citrate buffer (pH 6, 0.05% Tween20) for 15 min at 98°C. After blocking with 1% BSA sections were incubated with primary antibodies CD31 (Santa Cruz, 1:50; R&D, AF3628, 1:500) and SMA (Abcam, 1:100) over night. Sections were washed and Alexa 488 and Alexa 546 labeled secondary antibodies (Molecular Probes) were applied followed by a DAPI (Molecular Probes) staining. After mounting with Moviol (Calbiochem) samples were microscopically analyzed. Blood vessel structures were quantified blinded with image J and manual counting.

2.11. Real-time PCR

Total RNA was extracted using the RNeasy isolation kit (Qiagen, Hilden, Germany) with a prior proteinase K digestion (Qiagen, Hilden, Germany) and including a DNase treatment to remove residual genomic DNA. cDNA was prepared from equal amounts of total RNA using oligo(dT) primers and M-MLV reverse transcriptase (Promega, Madison, WI, USA). 10 ng of cDNA was amplified in a StepOnePlus™ Real-Time PCR System (Applied Biosystems) using TaqMan® Gene Expression Master Mix (Applied Biosystems) and appropriate probes (Applied Biosystems) (Table 2). cDNA levels were normalized to Rpl13a [31] and relative values were calculated using a respective calibrator. At least six independent samples were used for each condition.

3. Results

3.1. Characterization of PLL-g-PEG polymers

PLL-g-PEG forms stable nanocondensates with plasmid DNA, which successfully transfect cells *in vitro* [17]. To equip such polymers with additional features, we conjugated two specific peptides, namely polyR and TG (transglutaminase recognition sequence), to the distal end of the PEG molecules (Fig.1.B) in order to increase transfection efficiency or to covalently bind such polymers to a fibrin matrix, respectively. The size of DNA-polymer condensates critically determines the cellular uptake [16, 24, 32]. To predict the correlation of polymer modification with peptides and the polymer-DNA condensate size, we used dynamic light scattering (DLS) to measure the hydrodynamic diameter. In combination with DNA, unmodified PLL-g-PEG polymers form condensates with a mean diameter of 90 nm (Fig.2.A). Both modified polymers form spheric nanocondensates with hydrodynamic diameters of 102 and 112 nm respectively (Fig.2.A), suggesting that the condensate size is slightly affected by the peptide-functionalization. With an NH_4^+/PO_4^{3-} (N/P) ratio of 3.125, unmodified PLL-g-PEG condensates display an optimal compromise between high transfection efficiency and low cytotoxicity [17]. To determine the effect of the N/P ratio in peptide-linked polymer-DNA condensates, we analyzed the *in vitro* transcription efficiency in COS-7 cells using an enhanced GFP expressing vector (eGFP) (Fig.2.B). At N/P ratios of 3.125 or lower both, TG and polyR, modified polymers showed a poor transfection efficiency when compared to unmodified control polymers. With increasing N/P ratio of 6.25 or more, both polymers obtained improved transfection efficiency. TG-modified nancondensates (TG/GFP) reached similar transfection efficiencies when compared to unmodified nanocondensates (-/GFP) [17] and polyR-modified nanocondesates (polyR/GFP) exceeded the

transfection efficiency of -/GFP by factor 2. This indicates that the TG peptide does not negatively affect transfection whereas the polyR functionalization effectively enhances the transfection efficiency of PLL-g-PEG based nanocondesates. Since N/P ratios higher than 6.25 decrease cell survival [17], all further experiments were conducted with a N/P ratio of 6.25 for both, TG and polyR functionalized polymers, combining efficient transfection with low cytotoxicity as previously described [12, 16, 17].

To analyze whether diabetic conditions may influence the cellular uptake of PLL-g-PEG -DNA condensates, we pre-adapted COS-7 cells for four weeks in a high and low glucose environment to mimic diabetic and control conditions *in vitro* [30]. Our results indicate that the *in vitro* transfection efficiency of the different PLL-g-PEG polymers is comparable under high and low glucose conditions (Fig.2.C) suggesting that diabetes-like glucose levels have no effect on nanocondensate uptake. To predict the cytotoxicity of modified PLL-g-PEG polymers under high and low glucose conditions, we analyzed the cell viability of COS-7 cells. All different nanocondensates, with a N/P ratio of 6.25 for modified and a N/P ratio of 3.125 for unmodified polymers, display a high cell viability of 90 to 100% under both, normal and high glucose conditions (Fig.2.D).

Hence, the *in vitro* characterization of peptide-functionalized PLL-g-PEG polymers-DNA condensates suggests that such condensates have improved transfection efficiency and low cytotoxicity, which is independent of the glucose environment.

3.2. Release pattern of PLL-g-PEG polymers from fibrin matrices

To analyze whether TG functionalized PLL-g-PEG polymers are covalently incorporated into a 3D delivery network, we embedded PLL-g-PEG -TG/pEGFP-N1

(TG/GFP) (N/P 6.25) and PLL-g-PEG/pEGFP-N1 (-/GFP) (N/P 3.125) nanocondensates into fibrin matrices and monitored their release over a period of 7 days with naked DNA serving as a control. Nanocondensate-containing fibrin matrices were incubated with PBS and the release was quantified by DNA measurements to determine the release kinetics. Plain DNA and -/GFP were progressively released from fibrin matrices into the supernatant (Fig.3.A). With a relative release of 67% after 7 days, plain DNA displayed higher release kinetics than -/GFP with 46% after 7 days. In contrast, TG/GFP remained entrapped within the fibrin matrix suggesting that these nanocondensates were covalently incorporated. Additionally, the recognition and cross-linking of PLL-g-PEG -TG nanocondensates by factor XIIIa was confirmed by MAPL analysis (supplemental data Fig. 3).

To determine whether embedding into the fibrin matrix affects the integrity and functionality of PLL-g-PEG nanocondensates, we performed transfection studies with PBS supernatant containing the released nanocondensates. -/GFP was able to transfect COS-7 cells within the first 5 days (Fig.3.B) with 50% efficiency of non-embedded control samples suggesting that released nanocondensates remained intact. After day 6 the transfection efficiency was decreased which correlates with the reduced release of -/GFP nanocondensates at day 6 and 7. Released naked DNA and supernatants of TG/GFP containing matrices showed no transfection of COS-7 cells.

PLL-g-PEG nanocondensates can be successfully embedded into a 3D fibrin delivery matrix and maintain their functionality after progressive release.

3.3. Diabetes mellitus type I induction in rats

To test whether the treatment with different PLL-g-PEG -DNA condensates encoding a stable form of HIF-1α (HIF-1α–ΔODD) affects wound angiogenesis of normal and

diabetic rats we used streptozotocin (STZ) to induce diabetes mellitus type 1. Rats received either STZ (65 mg/kg) or a respective mock injection. STZ- but not Mock-treated animals showed rising levels of blood glucose between 3 and 5 days post injection – reaching and maintaining a plateau (supplemental data Fig. 3). Typically for diabetic rats, STZ-treated animals showed in addition reduced gain in body weight over the same time period (supplemental data Fig. 3). Both parameters showed that the diabetic phenotype was successfully established.

3.4. Gene expression after HIF-1α−ΔODD gene delivery

HIF-1α encodes for the primarily oxygen dependent regulated subunit of the hetero-dimeric transcription factor HIF-1, which controls angiogenesis among other physiological pathways.

To assess whether the delivery of stable HIF-1α−ΔODD with different PLL-g-PEG polymers affects gene expression, we analyzed mRNA levels of the typical HIF-1 downstream target gene *Vegf* (Fig.4.A first row diagrams) 3 and 7 days post surgery. With -/HIF condensates performing the best, all nanocondensates induced *Vegf* gene expression in Mock treated animals (1.5 to 2 fold) compared to fibrin only treated wounds (negative control) and $VEGF_{165}$ protein treated positive controls suggesting that HIF-1α−ΔODD was successfully delivered. In contrast, STZ treated animals showed only slightly induced Vegf mRNA levels. In addition, we analyzed the expression of genes especially expressed by cells giving rise to new blood vessels. *Pecam1* encodes for CD31 – a typical endothelial cell marker and *Acta2* encodes α-SMA – a marker for smooth muscle cells and myofibroblasts that are involved in wound contaction. *Pecam1* (Fig.4.A. second row of diagrams) was induced in Mock-treated animals by wound treatment with -/HIF, TG/HIF and polyR/HIF 3 and 7 days

after surgery. $VEGF_{165}$ protein application slightly induced *Pecam1* in Mock-treated wounds 7 but not 3 days after injury. Again, STZ-treated animals showed only a minor induction of gene expression 7 days after surgery. *Acta2* gene expression (Fig.4.A. third row) was slightly induced after nanocondensate treatment in Mock treated animals, but not after $VEGF_{165}$ protein delivery.

3.5. The angiogenic response to HIF-1α−ΔODD gene delivery

HIF-1α gene delivery has been shown to promote wound healing and angiogenesis [33]. Our newly established PLL-g-PEG -DNA condensates are able to successfully deliver a HIF-1α expression system *in vivo* to initiate differential expression of angiogenesis-related genes. To test whether wound revascularization can be improved by such a treatment we immunohistochemically visualized and quantified endothelial cells and smooth muscle cells (α-SMA positive) in wounds of Mock- and STZ-treated rats 3 and 7 days after surgery (Fig.5.A.). In 3-day-old wounds we observed neither a difference in endothelial cell number (CD31 positive) nor in smooth muscle cells when comparing fibrin treated control wounds with PLL-g-PEG-HIF-1α−ΔODD or $VEGF_{165}$ treated wounds (supplemental data Fig. 4). 7 days post surgery nanocondensate treatments seem to induce the number of CD31 positive endothelial cells to approximately 150% in Mock-treated animals, suggesting an accelerated recruitment and/or proliferation of endothelial cells (Fig.5.B a) under normal conditions. However, wounds of STZ-induced animals displayed even a minor reduction of CD31 signals after nanoncondensate treatment – especially in polyR/HIF treated wounds. In line with these findings, we found smooth muscle actin positive cells induced by the different polymer-DNA condensates in normal animals but not in diabetic animals (Fig.5.B b). Since both – endothelial cells and smooth muscle cells –

participate in blood vessel formation, we counted CD31/SMA double positive signals in order to quantify maturely formed blood vessels. We found that VEGF protein, a potent inducer of angiogenesis, rather reduced the number of blood vessels in wounds of healthy animals. Furthermore, we found no difference in double stained structures and hence no increased number of mature blood vessels in Mock- as well as in STZ-treated animals (Fig.5.B c) 7 days post injury although both markers – CD31 and SMA – were induced after polymer-DNA treatment. That suggests that the increased smooth muscle actin positive cells may be rather myofibroblasts cells in a transition state between fibroblasts and smooth muscle cells than mature smooth muscle cells participating in vessel formation. Due to the observed elevated number of endothelial cells – contributing to blood vessels – and potential myofibroblasts that may contribute to wound contractility, we also determined the total cell number per wound area (Fig.5.B d) as well as the wound thickness (Fig.5.B e). However, except for reduction in polyR/HIF treated wounds of diabetic animals we found that neither the polymer-DNA condensates nor VEGF protein affected the total cell number – and hence proliferation or migration, respectively – per wound area. Additionally, the wound thickness was hardly affected in Mock treated animals. Surprisingly, under diabetes mimicking conditions polyR/HIF as well as the positive control VEGF seemed to repress instead of accelerate wound contraction. This, in combination with the reduced blood vessels after $VEGF_{165}$ application (Fig.5.B c), suggests that higher levels of VEGF – either applied or endogenously expressed – may even interfere with wound healing.

3.6. The impact of HIF-1α−ΔODD gene delivery on the capillary network

Both, $VEGF_{165}$ protein application as well as polymer-HIF-1α-DNA condensates, are

able to successfully induce blood vessel precursor cells but fail to induce mature blood vessels 7 days post injury. To estimate whether nanocondensate-mediated HIF-1α−ΔODD delivery affects the capillary network formation, we measured the diameter of blood vessels 7 days after surgery. The majority of capillaries in fibrin only treated wounds had a diameter of 4 – 8 µm (Fig.6.A.) with an average of 7 µm (Fig.6.B.). $VEGF_{165}$- and both nanocondensate- (-/HIF and TG/HIF) treatments increased the prevalence of smaller capillaries ranging between 2 and 6 µm in Mock treated animals (Fig.6.A.) resulting in a smaller average diameter of 5.8 to 6.5 µm (Fig.6.B.). A similar effect was observed in STZ-injected animals after -/HIF and TG/HIF treatment. However, $VEGF_{165}$ protein application into wounds of STZ-injected animals had no effect on the average blood vessel diameter when compared to fibrin-control wounds (Fig.6.B.). Wounds treated with polyR/HIF showed neither under normal nor under diabetic conditions an effect on blood vessel size.

4. Discussion

Wound revascularization depends on the precisely balanced interplay of several proangiogenic growth factors like VEGF and PDGF [34] and on a proper growth factor gradient [35] to direct blood vessel growth. Therefore, a protein therapy might be disadvantageous because locally administered proteins experience rapid dilution and degradation processes [36], which may cause an inhomogeneous gradient. Instead of the local administration of expensive protein cocktails, we established and used a system to deliver therapeutic DNA encoding a modified version of the alpha subunit of HIF-1, which escapes normoxic degradation due to the lack of its oxygen-dependent degradation domain (ODD) [22]. HIF-1 controls the expression of several proteins required for the induction and correct assembly of blood vessels [18] and has been shown to improve wound healing [33, 37, 38]. Since excessive over-expression of the HIF-1α subunit may correlate with pathophysiological tissue alteration and cancer growth [39], it is essential to temporarily control the expression pattern and to adapt it to the demand of the clinical situation. Here we established a PLL-g-PEG polymer-based gene delivery system as a therapeutic approach to transiently and safely alter HIF-1α expression levels. We employed previously characterized PLL-g-PEG based polymer with an optimized balance of low cytotoxicity, stealth properties and high cellular DNA-nanocondensate uptake [16, 17] and modified them with surface-functionalizing peptides for an *in vivo* application. We characterized them *in vitro* and tested them *in vivo* to explore their therapeutic potential under normal and diabetic conditions in a wound healing study.

Pegylation provides stealth properties and the possibility to conjugate functional modules to distal moieties of nancondensates. The polymers were surface-functionalized with either a fusogenic peptide consisting of 6 arginine residues

(polyR) to facilitate cellular uptake and transport through cellular compartments or a factor XIIIa transglutaminase substrate (TG) sequence allowing a covalent incorporation into fibrin wound-healing matrices [33]. TG and PolyR functionalized PLL-g-PEG-DNA condensates displayed a hydrodynamic diameter of 102 to 112 nm, suggesting that the condensates were slightly bigger than non-modified PLL-g-PEG-DNA condensates (90 nm) [17] but still displayed an appropriate size for cellular uptake [24, 32]. The nuclear uptake facilitating polyR peptide modification of PLL-g-PEG (N/P 6.25) improved the transfection rate of factor 2 *in vitro* when compared to unmodified PLL-g-PEG nanocondensates. The TG peptide covalently bound to fibrin and allows fibrin-embedded PLL-g-PEG–DNA condensates to remain entrapped within the matrix until matrix degradation occurs without losing their transfection efficiency. Both peptide modified PLL-g-PEG condensates displayed low cytotoxicity comparable to unmodified polymers [17]. Furthermore, unmodified and modified polymers maintained their transfection efficiency of COS-7 cells in a high glucose environment suggesting that a potential diabetic environment may not alter cellular uptake.

PLL-PEG nanocondensates have been shown to successfully deliver therapeutic plasmid DNA *in vivo* [40]. We employed our different PLL-g-PEG condensates *in vivo* to explore their pro-angiogenic therapeutic potential in a diabetic wound-healing model [41]. To progressively release the nanocondensates to the side of injury, we used fibrin matrices and embedded functionalized PLL-g-PEG polymers that condensed HIF-1α–ΔODD [22] plasmid DNA. Analyzing mRNA gene expression after wound treatment, we found that the HIF-1 downstream target gene *Vegf* was induced by polymer-DNA condensates in wounds of non-diabetic animal 3 and 7 days post injury. Especially unmodified PLL-g-PEG and PLL-g-PEG-TG polymers

displayed elevated *Vegf* mRNA levels indicating that HIF-1α was successfully delivered to the side of injury. The fact that the expression levels returned back to normal levels at a later stage of wound healing (7 days; Fig.4.) indicates that HIF-1α is indeed only transiently induced and experiences a progressive down regulation. PolyR modified PLL-g-PEG polymers, which showed the best transfection efficiency *in vitro*, induced the *Vegf* mRNA expression *in vivo* but did not further improve the elevated expression levels of unmodified or TG-modfied nanocondensates. In contrast to healthy animals, the nanocondensates failed to significantly induce *Vegf* gene expression in diabetic animals, although high glucose adapted COS-7 cells showed no reduced nanocondensate uptake *in vitro*. It seems that HIF-1α, although a sustained expression can improve wound healing and revascularization in normal [33] and diabetic mice [42], is more rapidly degraded [43] and displays a reduced activity under hyperglycemic conditions [30, 44] due to the methylglyoxylation of its transcriptional cofactor p300. In concordance, we observed that *Pecam1* and *Acta2*, which encode the blood vessel markers CD31 and α-SMA [45, 46], were induced in healthy animals 3 and 7 days after wounding after condensate application but less pronounced in diabetic animals. Released $VEGF_{165}$ protein – a potent inducer of endothelial cell proliferation and recruitment [45] – seems to be rapidly diluted and degraded [36] and hardly affects Pecam1 expression levels.

In line with the mRNA expression data, we found that HIF-1α delivery by PLL-g-PEG nanocondensates resulted in an increased migration or proliferation of CD31 and α-SMA positive cells – that give rise to mature blood vessels – in control but not in diabetes type I resembling rats. However, we could not detect any increased mature blood vessel structures upon HIF-1α gene or VEGF protein delivery. Fibrin *per se* has wound healing properties [47] and it might be possible that fibrin masks the effect of

wound revascularization after HIF-1α gene delivery. Nevertheless, the elevated levels of endothelial cells and α-SMA positive cells suggest that the wounds respond with a preliminary angiogenic response to the polymer-DNA condensates without forming increased mature blood vessels structures at the time points of analyzes. However, due to the severe toxicity of STZ the experiment was always terminated at the latest 7 days after wounding and no later time points were analyzed. In addition to blood vessel quantification, we measured the diameter of the blood vessels to predict the quality of the vascular network. In contrast to polyR-modified polymers, blood vessels of PLL-g-PEG and PLL-g-PEG-TG polymer treated wounds had a smaller average diameter than fibrin controls, suggesting that they faster developed an advanced capillary system. $VEGF_{165}$ protein treatment caused a reduced capillary diameter in control animals, suggesting that it might be able to fine-tune the capillary network. However, this effect was abolished under hyperglycemic conditions and confirms other studies [45], where it was reported that VEGF might be disadvantageous for diabetic wound healing due to the formation of non-physiologically leaky vessels, which can cause hemorrhage [48].

5. Conclusion

PLL-g-PEG polymers condense plasmid DNA and can be functionalized with different peptides to modify their properties. The PLL-g-PEG dependent delivery of an oxygen-insensitive variant of HIF-1α *in vivo* successfully leads to differential gene expression and initiates an incipient angiogenic response in cutaneous wounds. However, we observed reduced effects in diabetic animals, possibly due to the hyperglycemia-dependent, reduced HIF-1α activity. Nanocondensates modified with polyR showed strongly improved transfection efficiency *in vitro* but not *in vivo*. In

fact, the inhibited wound contraction and the lack of capillary tuning indicate that it may even hinder wound healing under diabetic conditions. The wound milieu displays a much more complex environment and less controllable conditions than an *in vitro* assay and our results indicate that *in vitro* data have to be carefully considered since they do not necessarily predict the systemic environment of *in vivo* situations. It is convenient to establish and to test DNA delivering polymers or other systems *in vitro* but it is essential to verify these approaches in animal studies and to adapt them in order to match the requirements for a proper *in vivo* application. Furthermore, our diabetes model was toxin-induced and our studies had to be done on a narrow time frame, although diabetes is a chronic disease and may require long-term studies.

Acknowledgements

The authors thank Prof. Viola Vogel and her group for constant support and excellent scientific discussions. Dr. Thomas C. Weber and Joerg Fehr are acknowledged for their kind input and support during the animal studies. This work was supported by the Swiss National Science Foundation (SNF, grant 127585).

References

[1] Gurtner GC, Werner S, Barrandon Y, Longaker MT. Wound repair and regeneration. Nature. 2008;453:314-21.

[2] Blakytny R, Jude EB, Martin Gibson J, Boulton AJ, Ferguson MW. Lack of insulin-like growth factor 1 (IGF1) in the basal keratinocyte layer of diabetic skin and diabetic foot ulcers. J Pathol. 2000;190:589-94.

[3] Whitney JD. Wound care: the challenges ahead. Rehabil Nurs. 2005;30:78-9.

[4] Gary Sibbald R, Woo KY. The biology of chronic foot ulcers in persons with diabetes. Diabetes Metab Res Rev. 2008;24 Suppl 1:S25-30.

[5] Kuehn BM. Chronic wound care guidelines issued. JAMA. 2007;297:938-9.

[6] Chandler LA, Gu DL, Ma C, Gonzalez AM, Doukas J, Nguyen T, et al. Matrix-enabled gene transfer for cutaneous wound repair. Wound Repair Regen. 2000;8:473-9.

[7] Eriksson E, Velander P. Gene transfer in wound healing. Br J Surg. 2004;91:1093-4.

[8] Keswani SG, Katz AB, Lim FY, Zoltick P, Radu A, Alaee D, et al. Adenoviral mediated gene transfer of PDGF-B enhances wound healing in type I and type II diabetic wounds. Wound Repair Regen. 2004;12:497-504.

[9] Tal J. Adeno-associated virus-based vectors in gene therapy. J Biomed Sci. 2000;7:279-91.

[10] Ramsay E, Hadgraft J, Birchall J, Gumbleton M. Examination of the biophysical interaction between plasmid DNA and the polycations, polylysine and polyornithine, as a basis for their differential gene transfection in-vitro. Int J Pharm. 2000;210:97-107.

[11] Halama A, Kulinski M, Librowski T, Lochynski S. Polymer-based non-viral gene delivery as a concept for the treatment of cancer. Pharmacol Rep. 2009;61:993-9.

[12] von Erlach T, Zwicker S, Pidhatika B, Konradi R, Textor M, Hall H, et al. Formation and characterization of DNA-polymer-condensates based on poly(2-methyl-2-oxazoline) grafted poly(L-lysine) for non-viral delivery of therapeutic DNA. Biomaterials. 2011;32:5291-303.

[13] Zaitsev S, Cartier R, Vyborov O, Sukhorukov G, Paulke BR, Haberland A, et al. Polyelectrolyte nanoparticles mediate vascular gene delivery. Pharm Res. 2004;21:1656-61.

[14] Lee H, Jeong JH, Park TG. PEG grafted polylysine with fusogenic peptide for gene delivery: high transfection efficiency with low cytotoxicity. J Control Release. 2002;79:283-91.

[15] Choi YH, Liu F, Kim JS, Choi YK, Park JS, Kim SW. Polyethylene glycol-grafted poly-L-lysine as polymeric gene carrier. J Control Release. 1998;54:39-48.

[16] Luhmann T, Rimann M, Bittermann AG, Hall H. Cellular uptake and intracellular pathways of PLL-g-PEG-DNA nanoparticles. Bioconjug Chem. 2008;19:1907-16.

[17] Rimann M, Luhmann T, Textor M, Guerino B, Ogier J, Hall H. Characterization of PLL-g-PEG-DNA nanoparticles for the delivery of therapeutic DNA. Bioconjug Chem. 2008;19:548-57.

[18] Weidemann A, Johnson RS. Biology of HIF-1alpha. Cell Death Differ. 2008;15:621-7.

[19] Bruick RK, McKnight SL. A conserved family of prolyl-4-hydroxylases that modify HIF. Science. 2001;294:1337-40.

[20] Jaakkola P, Mole DR, Tian YM, Wilson MI, Gielbert J, Gaskell SJ, et al. Targeting of HIF-alpha to the von Hippel-Lindau ubiquitylation complex by O2-regulated prolyl hydroxylation. Science. 2001;292:468-72.

[21] Masson N, Willam C, Maxwell PH, Pugh CW, Ratcliffe PJ. Independent function of two destruction domains in hypoxia-inducible factor-alpha chains activated by prolyl hydroxylation. EMBO J. 2001;20:5197-206.

[22] Huang LE, Gu J, Schau M, Bunn HF. Regulation of hypoxia-inducible factor 1alpha is mediated by an O2-dependent degradation domain via the ubiquitin-proteasome pathway. Proc Natl Acad Sci U S A. 1998;95:7987-92.

[23] Mahon PC, Hirota K, Semenza GL. FIH-1: a novel protein that interacts with HIF-1alpha and VHL to mediate repression of HIF-1 transcriptional activity. Genes Dev. 2001;15:2675-86.

[24] Trentin D, Hubbell J, Hall H. Non-viral gene delivery for local and controlled DNA release. J Control Release. 2005;102:263-75.

[25] Currie LJ, Sharpe JR, Martin R. The use of fibrin glue in skin grafts and tissue-engineered skin replacements: a review. Plast Reconstr Surg. 2001;108:1713-26.

[26] Montano I, Schiestl C, Schneider J, Pontiggia L, Luginbuhl J, Biedermann T, et al. Formation of human capillaries in vitro: the engineering of prevascularized matrices. Tissue Eng Part A. 2010;16:269-82.

[27] Mogford JE, Tawil B, Jia S, Mustoe TA. Fibrin sealant combined with fibroblasts and platelet-derived growth factor enhance wound healing in excisional wounds. Wound Repair Regen. 2009;17:405-10.

[28] Catelas I, Dwyer JF, Helgerson S. Controlled release of bioactive transforming growth factor beta-1 from fibrin gels in vitro. Tissue Eng Part C Methods. 2008;14:119-28.

[29] Pasche S, Textor M, Meagher L, Spencer ND, Griesser HJ. Relationship between interfacial forces measured by colloid-probe atomic force microscopy and protein resistance of poly(ethylene glycol)-grafted poly(L-lysine) adlayers on niobia surfaces. Langmuir. 2005;21:6508-20.

[30] Thangarajah H, Yao D, Chang EI, Shi Y, Jazayeri L, Vial IN, et al. The molecular basis for impaired hypoxia-induced VEGF expression in diabetic tissues. Proc Natl Acad Sci U S A. 2009;106:13505-10.

[31] Wood SH, Clements DN, McEwan NA, Nuttall T, Carter SD. Reference genes for canine skin when using quantitative real-time PCR. Vet Immunol Immunopathol. 2008;126:392-5.

[32] Park TG, Jeong JH, Kim SW. Current status of polymeric gene delivery systems. Adv Drug Deliver Rev. 2006;58:467-86.

[33] Trentin D, Hall H, Wechsler S, Hubbell JA. Peptide-matrix-mediated gene transfer of an oxygen-insensitive hypoxia-inducible factor-1alpha variant for local induction of angiogenesis. Proc Natl Acad Sci U S A. 2006;103:2506-11.

[34] Hao X, Silva EA, Mansson-Broberg A, Grinnemo KH, Siddiqui AJ, Dellgren G, et al. Angiogenic effects of sequential release of VEGF-A165 and PDGF-BB with alginate hydrogels after myocardial infarction. Cardiovasc Res. 2007;75:178-85.

[35] Gerhardt H, Golding M, Fruttiger M, Ruhrberg C, Lundkvist A, Abramsson A, et al. VEGF guides angiogenic sprouting utilizing endothelial tip cell filopodia. J Cell Biol. 2003;161:1163-77.

[36] Hendel RC, Henry TD, Rocha-Singh K, Isner JM, Kereiakes DJ, Giordano FJ, et al. Effect of intracoronary recombinant human vascular endothelial growth factor on myocardial perfusion: evidence for a dose-dependent effect. Circulation. 2000;101:118-21.

[37] Botusan IR, Sunkari VG, Savu O, Catrina AI, Grunler J, Lindberg S, et al. Stabilization of HIF-1alpha is critical to improve wound healing in diabetic mice. Proc Natl Acad Sci U S A. 2008;105:19426-31.

[38] Albina JE, Mastrofrancesco B, Vessella JA, Louis CA, Henry WL, Jr., Reichner JS. HIF-1 expression in healing wounds: HIF-1alpha induction in primary inflammatory cells by TNF-alpha. Am J Physiol Cell Physiol. 2001;281:C1971-7.

[39] Stoeltzing O, McCarty MF, Wey JS, Fan F, Liu W, Belcheva A, et al. Role of hypoxia-inducible factor 1alpha in gastric cancer cell growth, angiogenesis, and vessel maturation. J Natl Cancer Inst. 2004;96:946-56.

[40] Walsh M, Tangney M, O'Neill MJ, Larkin JO, Soden DM, McKenna SL, et al. Evaluation of cellular uptake and gene transfer efficiency of pegylated poly-L-lysine compacted DNA: implications for cancer gene therapy. Mol Pharm. 2006;3:644-53.

[41] Kwon AH, Qiu Z, Hashimoto M, Yamamoto K, Kimura T. Effects of medicinal mushroom (Sparassis crispa) on wound healing in streptozotocin-induced diabetic rats. Am J Surg. 2009;197:503-9.

[42] Mace KA, Yu DH, Paydar KZ, Boudreau N, Young DM. Sustained expression of Hif-1alpha in the diabetic environment promotes angiogenesis and cutaneous wound repair. Wound Repair Regen. 2007;15:636-45.

[43] Catrina SB, Okamoto K, Pereira T, Brismar K, Poellinger L. Hyperglycemia regulates hypoxia-inducible factor-1alpha protein stability and function. Diabetes. 2004;53:3226-32.

[44] Thangarajah H, Vial IN, Grogan RH, Yao D, Shi Y, Januszyk M, et al. HIF-1alpha dysfunction in diabetes. Cell Cycle. 2010;9:75-9.

[45] Ilan N, Madri JA. PECAM-1: old friend, new partners. Curr Opin Cell Biol. 2003;15:515-24.

[46] Skalli O, Pelte MF, Peclet MC, Gabbiani G, Gugliotta P, Bussolati G, et al. Alpha-smooth muscle actin, a differentiation marker of smooth muscle cells, is present in microfilamentous bundles of pericytes. J Histochem Cytochem. 1989;37:315-21.

[47] Drew AF, Liu H, Davidson JM, Daugherty CC, Degen JL. Wound-healing defects in mice lacking fibrinogen. Blood. 2001;97:3691-8.

[48] Alfranca A. VEGF therapy: a timely retreat. Cardiovasc Res. 2009;83:611-2.

Tables

Table 1. Nomenclature and abbreviation of the different PLL-g-PEG-DNA condensates

Polymer	DNA	Nomenclature	Label
PLL-g-PEG	pEGFP-N1	PLL-g-PEG/pEGFP-N1	-/GFP
PLL-g-PEG-TG	pEGFP-N1	PLL-g-PEG-TG/pEGFP-N1	TG/GFP
PLL-g-PEG-polyR	pEGFP-N1	PLL-g-PEG-polyR/pEGFP-N1	polyR/GFP
PLL-g-PEG	pHIF-1α–ΔODD	PLL-g-PEG/pHIF-1α–ΔODD	-/HIF
PLL-g-PEG-TG	pHIF-1α–ΔODD	PLL-g-PEG-TG/pHIF-1α–ΔODD	TG/HIF
PLL-g-PEG-polyR	pHIF-1α–ΔODD	PLL-g-PEG-poyR/pHIF-1α–ΔODD	polyR/HIF

Table 2. Taq Man probes used for real-time PCR

Gene	Probe
Rpl13a	Rn00821946_g1
Pecam1 (CD31)	Rn01467262_m1
Acta2 (SMA)	Rn01759928_g1
Vegf	Rn01511601_m1

Table 3. Primary Antibodies

Target	Name	Supplier	Dilution
CD31	AF3628	R&D	1:500
SMA	ab5694	Abcam	1:500
VEGF	MAB293	R&D	1:400
b-Actin	ab8227	Abcam	1:1000

Figures

Fig.1. Composition and structure of different PLL-g-PEG polymers. **A** PLL-g-PEG polymers consist of a 20 kDa PLL backbone, which is grafted by PEG with a ratio ranging between 3 and 8%. Surface-functionalized polymers carry peptides, namely TG and polyR, at the distal end of PEG. **B** Schematic view of PLL-g-PEG polymers with the lysine backbone (blue) consisting of 96 residues, the 5 kDa PEG residue (red) and both TG and polyR peptides (yellow) shows, that the peptides bind to PEG-maleimide via a the available sulfhydryl group of cysteine.

Fig.2. Characterization of different PLL-g-PEG-DNA condensates. **A** The hydrodynamic diameter of different PLL-g-PEG polymers PLL-g-PEG/pEGFP (-/GFP), PLL-g-PEG-TG/pEGFP (TG/GFP) and PLL-g-PEG-polyR/pEGFP (polyR/GFP) condensates was determined by dynamic light scattering and varied between 90 and 112 nm (n = 3). **B** The transfection efficiency of PLL-g-PEG-TG/pEGFP (TG/GFP) and PLL-g-PEG-polyR/pEGFP (polyR/GFP) condensates was assessed in COS-7 cells with different N/P ratios from 1 to 25 by normalizing to the transfection efficiency of unmodified PLL-g-PEG/pEGFP condensates (N/P 2.125); shown are means of triplicates ± Stdv. **C** The transfection efficiency of PLL-g-PEG polymers PLL-g-PEG/pEGFP (-/GFP), PLL-g-PEG-TG/pEGFP (TG/GFP) and PLL-g-PEG-polyR/pEGFP (polyR/GFP) condensates in COS-7 cell under normal (1 g/l) and high (4.5 g/l) glucose conditions. Values were normalized to -/GFP under normal conditions; shown are means of triplicates ± Stdv. **D** The cell viability was assessed for PLL-g-PEG polymers PLL-g-PEG/pEGFP (-/GFP), PLL-g-PEG-TG/pEGFP (TG/GFP) and PLL-g-PEG-polyR/pEGFP (polyR/GFP) condensates in COS-7 cell using a WST-1 assay under normal (1 g/l) and high (4.5 g/l) glucose conditions. Values were normalized to untreated negative controls; shown are means of triplicates ± Stdv.

Fig.3. *In vitro* DNA and nanocondensate release from 3D fibrin matrices. **A** The release of PLL-g-PEG (-/GFP) and PLL-g-PEG-TG (TG/GFP) polymer-DNA condensates from 3D fibrin matrices was monitored for 7 days and PBS supernatant was removed and replaced in a 24-hour cycle The cumulative, relative values were obtained by adding the daily measured DNA content and normalizing them to the total DNA amount initially embedded within the fibrin matrix. Naked DNA served as a negative control; shown are means of triplicates ± Stdv. **B** The released DNA containing PLL-g-PEG (-/GFP) and PLL-g-PEG-TG (TG/GFP) condensates as well as released naked DNA in the daily isolated supernatant was used to transfect COS-7 cells. All values were normalized to non-embedded PLL-g-PEG/EGFP condensate-controls containing 1 µg DNA; shown are means of triplicates ± Stdv.

Fig.4. Expression of HIF-1 target gene *Vegf* and the pro-angiogenic markers *Pecam1* and *Acta2* during *in vivo* wound healing. mRNA levels were determined 3 and 7 days post injury in wounds of normal (Mock) and diabetic (STZ) rats. Wounds were filled with either empty fibrin matrices (Fibrin – negative control), $VEGF_{165}$ containing fibrin matrices ($VEGF_{165}$ positive control) or with the different nanocondensates containing fibrin matrices: PLL-g-PEG/pHIF-1α-ΔODD (-/HIF), PLL-g-PEG-TG/pHIF-1α-ΔODD (TG/HIF) and PLL-g-PEG-polyR/pHIF-1α-ΔODD (polyR/HIF). Rpl13a served as reference gene and expression levels were normalized to fibrin negative controls for each individual animal. Shown are means of 6 n ± SEM. Statistical validations were performed using a one-sample Wilcoxon signed rank test; * ≤ 0.05.

Fig.5. Quantification of vascular structures during wound healing. Wounds of normal (Mock) and streptozotocin treated (STZ) rats were treated with fibrin only (negative control), with fibrin embedded $VEGF_{165}$ (positive control) or with different fibrin embedded nanocondensates: PLL-g-PEG/pHIF-1α-ΔODD (-/HIF), PLL-g-PEG-TG/pHIF-1α-ΔODD (TG/HIF) and PLL-g-PEG-polyR/pHIF-1α-ΔODD (polyR/HIF). **A** Shown are representative, centrally located sections of wound-cross-sections used for quantification 7 days after injury. Immunofluorescence staining indicates CD31 positive endothelial cells (red), a-SMA positive smooth muscle actin positive cells (green) and total number of cells (DAPI, blue). Scale bar: 250 µm. **B** Quantification of vascular structures and precursors in centrally located sections of wound-cross-sections 7 days after injury. Upper panel shows the number of positive CD31 endothelial cells (left), a-SMA positive cells (middle) and CD31/SMA counts (right) normalized to the analyzed area. The lower panel represents the number of total cells (DAPI) per analyzed wound area (left) and the wound diameter (right). For all analyzes, values were normalized to fibrin negative controls for each animal and shown are means of triplicates ± SEM. Statistical validations were performed using a one-sample t- test; * ≤ 0.05.

Fig.6. Estimation of the blood vessel diameter during wound healing in normal (Mock) and diabetic (STZ) rats 7 days after injury. The vessel diameter was measured in the central region of wound-cross-sections either treated with fibrin only (negative control), with fibrin embedded $VEGF_{165}$ (positive control) or with different fibrin embedded nanocondensates: PLL-g-PEG/pHIF-1α-ΔODD (-/HIF), PLL-g-PEG-TG/pHIF-1α-ΔODD (TG/HIF) and PLL-g-PEG-polyR/pHIF-1α-ΔODD (polyR/HIF). **A** Shown are representative histograms of two individual rats (Mock vs. diabetic) and the distribution of the blood vessel diameter in the differently treated wounds. The x-axis represents the blood vessel size from 1 µm to 19 µm plus the last bar summarizing all vessels with a size of 20 or more µm. The relative blood

vessel amount was determined with “number of vessels per group” over “total number of analyzed blood vessels” (approximately 90 -150 per wound). **B** Shown is the mean of the average blood vessel diameter of 3 individual rats ± Stdv. Statistical validations were performed using a t- test comparing samples of both groups (Mock and STZ) against their respective fibrin negative control; * ≤ 0.05.

A

Nomenclature	PLL (kDa)	PEG (kDa)	PEG grafting density g [%]	Functionalizing Peptide
PLL_{20}-g_5-PEG_5	20 kDa	5 kDa	5 %	
PLL_{20}-g_8-PEG_5-TG	20 kDa	5 kDa	8 %	**TG**: NQEQVSPLGYERCG
PLL_{20}-g_3-PEG_5-polyR	20 kDa	5 kDa	3 %	**polyR**: RRRRRRRGYGRRC

B

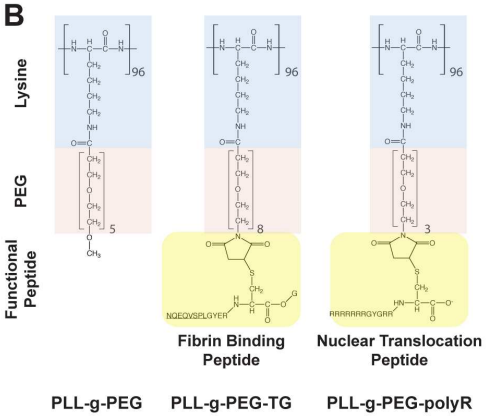

A

Polymercondensate	Hydrodynamic Diameter [nm]
-/GFP	90 ± 2
TG/GFP	102 ± 3.9
polyR/GFP	112 ± 16.8

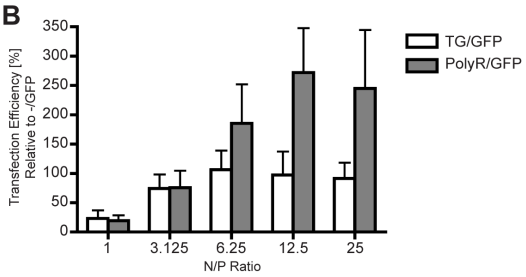

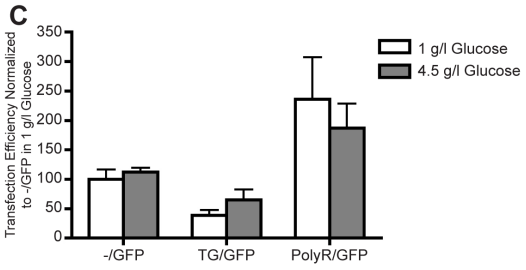

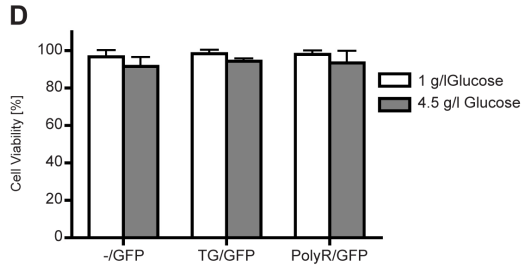

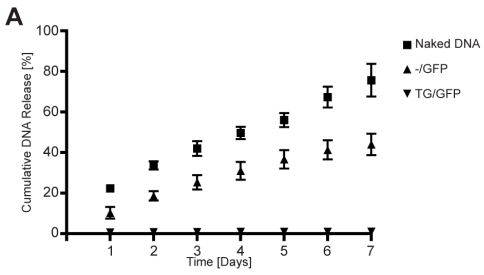
A
Cumulative DNA Release [%]
100
80
60
40
20
0
1
2
3
4
5
6
7
Time [Days]
Naked DNA
-/GFP
TG/GFP

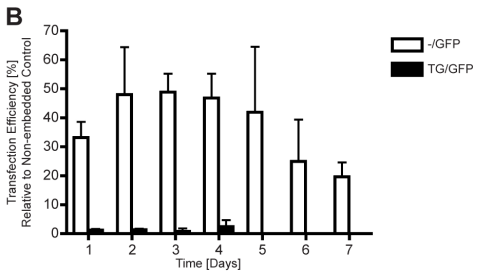
B
Transfection Efficiency [%]
Relative to Non-embedded Control
70
60
50
40
30
20
10
0
1
2
3
4
5
6
7
Time [Days]
-/GFP
TG/GFP

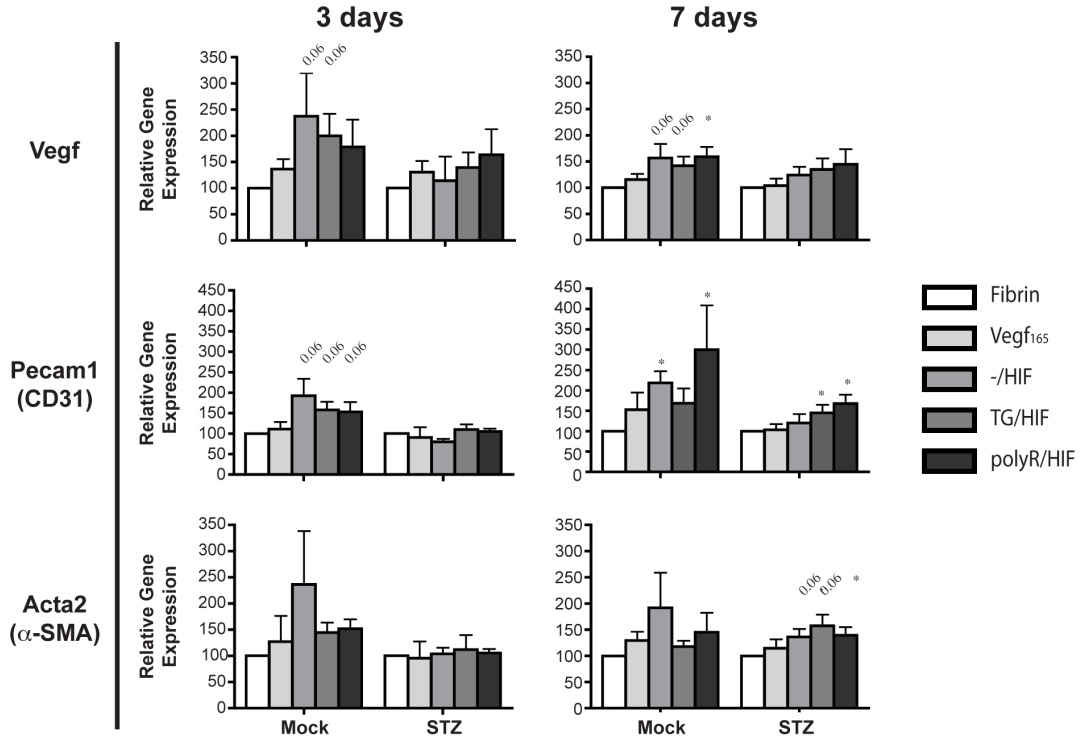
3 days
7 days
Vegf
Pecam1 (CD31)
Acta2 (α-SMA)
Relative Gene Expression
0.06
*
Mock
STZ
Fibrin
Vegf165
-/HIF
TG/HIF
polyR/HIF

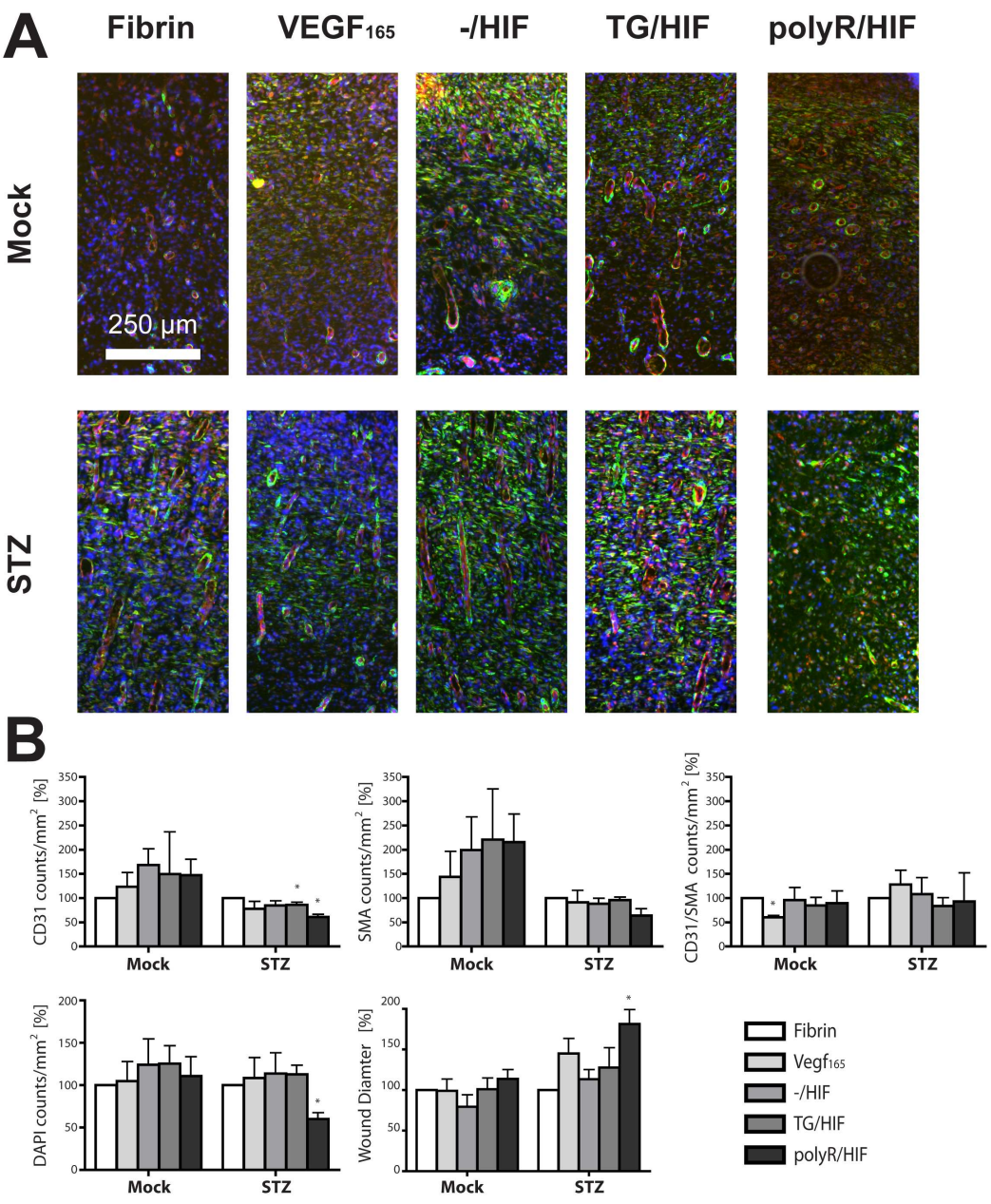
A
Fibrin
VEGF165
-/HIF
TG/HIF
polyR/HIF
Mock
STZ
250 µm
B
CD31 counts/mm2 [%]
SMA counts/mm2 [%]
CD31/SMA counts/mm2 [%]
DAPI counts/mm2 [%]
Wound Diamter [%]
Mock
STZ
Fibrin
Vegf165
-/HIF
TG/HIF
polyR/HIF

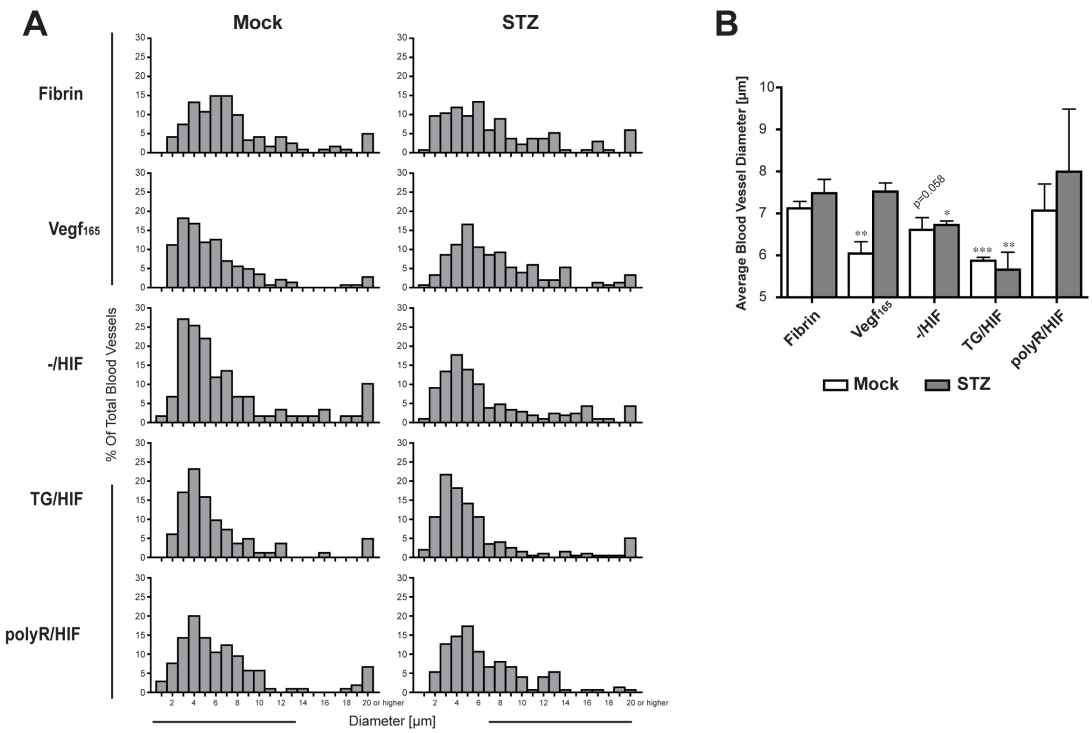
A
Mock
STZ
Fibrin
Vegf165
-/HIF
TG/HIF
polyR/HIF
% Of Total Blood Vessels
Diameter [µm]
B
Average Blood Vessel Diameter [µm]
p=0.058
Mock
STZ